AEROELASTICITY OF A COAXIAL HELICOPTER ROTOR

Doctor B.N. BURTSEV

Kamov Helicopter Scientific & Technology Company

USSR

Abstract

The development results of the coaxial-rotor lifting system generalized mathematical model are discussed. The coaxial-rotor system is modeled by means of aeroelastic blade couplings through signal control links and also by aeroelastic blade interaction in coaxial rotor vortex. An unlinear blade vortex model is developed on the basis of lifting surface theory to model this phenomenon. The functional capabilities consist in modeling either stationary or unstationary modes of flight. Either modeling of forced rotor blade motion or modeling of aeroelastic unstability flutter are possible. The available analysis results consist in possibility to reflect, within the limits of a single model, upper and lower rotor blade loads and deformations, signal control links loads and deformations, flapping motion and aeroelastic blade approach.

The numerical method and algorithm development results are presented.

The stall flutter, flutter, coaxial-rotor system blade approach study results obtained in numerical experiments are given.

The flight test support and analysis results on the basis of mathematical model are discussed. The flight tests fully proved the validity of the solutions while designing a new rotor system. The aeroelastical design arrangement parameters influence on the loads and vibration is studied in flight experiments, and the aeroelastic blade layout is considerably improved.

The design, flight testing and development of coaxial helicopters at the Kamov Design Bureau is done on the basis of scientific studies and solving the problems on the coaxial-rotor system aeroelasticity. By aeroelasticity problems the auther means a complex of interconnected tasks shown on fig.1. This report presents a summary of a longstanding experience of Kamov Company and because of the large amount of the material only the breif survey of the main results is given.

1. THE COAXIAL-ROTOR SYSTEM GENERAL MATHEMATICAL MODEL

A general mathematical model of coaxial-rotor system is developed. The coaxial-rotor system is modeled by elastic blade couplings through the control linkage as well as by an aeroelastic blades interaction in the coaxial-rotor vortex wake. The functional capabilities permit to model both stationary and non-stationary flight modes and it is also possible to model forced rotor blade motions as well as an aeroelastic instability of a flutter type. The results of the study enable us to show, within the frames of a common mode, the loads and deformations of the upper and lower rotor blades, loads and deformations of the control linkage, flapping motion and approach of elastic blades. The blade motion equations system and the boundary conditions are shown on fig.2. The motion equations are obtained by the author nith the use of the minimal action principle (in Hamilton form). The blade is presented as a beam elastic for bending and torsion. The centre of mass, the centre of normal streching force application, the centre of torsion in blade sections need not coinside. The boundary conditions model nonlinear and periodic conditions on bending as well as a joint blade roots torsion on an elastic control linkage.

The necessity to study the rigid characteristics of the rotors control linkage is determined by the increase of deformations due to the increase of the blade pitch link loads in the maximum speed and overload modes, i.e. the limit flight modes.

The main results of the study consist in the development of the metodology and in the experimental determination of the control linkage elasticity matrix-functions for full scale coaxial helicopters of four types. The analysis of the experimental results permited to work out a control linkage mathematical model and a corresponding formula for the "approximation-calculation" of the matrix-function elements. With the help of this formula the rigidity characteristics of the control linkage aggregates were determined without their physical measuring for coaxial helicopters of four types. It is demonstrated that the eigenvectors of the elastisity matrix are actually blade torsional modes on the control linkage and the eigenvalues are actually linkage "dynamic elasticities" of the corresponding mode which are usually determined in a different way - that is by the linkage frequency testing. The study results are illustrated on fig. 3.

The air loads of the blade element model the set of aerodynamic processes:

- the "dynamic stall" which is modeled by approximation of the wind-tunnel testing results on the airfoils which oscillate on stalling and beyond stalling angles of attack;

- aeroelastic deformations of the blade trailing section airfoil countour;

- compressibility and stall which are modeled on the basis of the wind-tunnel test results in steady flow.

The method is proposed and the aerodynamic characteristics of an aeroelastic deformed airfoil are obtained on the basis of the wind-tunnel test results of a "rigid" airfoil in a steady flow and pressure, force and moments calculations in transonic flow on a rigid and "elastic" airfoil proposed by A.A. Nikolsky (TSAGI,the Central Aerodynamics Institute of the USSR).

The main features of the unsteady blade loads calculations are shown on fig.4.

Another most important physical factor determining the unsteady air loads is the blades inductive interaction in the coaxial-rotor vortex wake. A nonlinear vortex blade model was worked out on the basis of the lifting surface theory to model this phenomenon. The most peculier feature is the solving of a linear algebraic equations system determining the solid-wall-boundary condition at the aeroelastically deformed lifting surfaces (blades) together with motion equations integrating. The blade flap, lag and torsion deformations and common elastic blade turns on the control linkage are taken into account at the calculation. Thus the correspondence of momentary deformations, blade air loads and the intensities of lifting and free vortex surfaces presenting the coaxial-rotor vortex system, is obtained. The vortex model admits a random unsteady helicopter motion. The nonlinear (noncylindrical) vortex wake form depends upon the flying speed and obtained by approximating the results of a Mi-4 helicopter rotor tip wake smoke visualization (this experiment was made at LII, the Flight Testing Institute of the USSR). The vortex model developed is shown on fig.5.

Making a summary it may be said that creating of general mathematical model demanded a thorough development of a coaxial-rotor lifting system aeroelasticity main problems, i.e. motion equations, boundary conditions, air load calculation methods, vortex blade model for coaxial-rotor.

2. THE NUMERICAL METHOD AND ALGORITHM

Numerical methods and algorithms implementing the general mathematical model were developed. There was obtained a closed numerical solution of a differential equations system describing the coaxial-rotor blade motion and an algebraic equations system for the solid-wall-boundary condition at the deformed lifting surfaces.

3. THE NUMERICAL EXPERIMENT

Some results of the study and the coaxial-rotor lifting system aeroelasticity problems solving on the basis of the general mathematical model are given below. The functional capabilities and the modeled factors are illustrated on fig.7. Each of the fig.7 table column corresponds to one of the methods (algorithms). The most complete basic algorithm is designated "ULYSS-6", it embraces all the factors and models the coaxial-rotor lifting system (CRLS) in general. Other algorithms model only an isolated blade (B) and are used to solve some separate problems.

Calculation results correspond quite satisfactory to the flight test results and the influence of several factors connected with the model novelty is analysed. The results are illustrated on fig.6. It should also be noted that it is possible to calculate constant and variable loads on the control linkage with the help of the model.

The phenomenon of the stall flutter limits the helicopter performance in the coordinates of speed-altitude-overload. Without proper knowledge of this limitation and without its prediction it is not possible to choose correctly the main parameters of the lifting system i.e. rotor diameter, tip speed, blade chord, number of blades.

Some capabilities of the model are shown on fig.8. It is namely a satisfactory correlation with the flight test results on the dependence of the pitch link loads form the azimuth, the increase of the amplitude depending upon the overload and the character of increase. It may be seen that the calculation of a single blade overestimates the available helicopter overload.

Both in aeroelastic blade calculation and in the flight test results analysis the stall boundary is taken to be the dependence $C_T/\bar{\sigma} = f(\bar{V})$, to which correspond the pitch link loads amplitude values 60...70 kgm. The allowable values of pitch link loads are determined by the dynamic strength of the lifting system aggregates.

For the first time there was obtained a calculated stall flutter boundary for an isolated blade elastic for bending and torsion as well as for coaxial-rotor lifting system. From the qualitative and quantitative point of view this boundary differs from the stall boundary of the rigid blade. It is seen that the boundary may look as a "wall" with respect to the flying speed. The dependences of the boundary upon the rigidity of the control linkage and a helicopter drag (connected with the rotor angle of attack) were examined. It is shown that with the decrease of the helicopter drag the stall boundary is essentially brought farther with respect to the speed and changes its shape. Comparison with flight experiment shows that the model describes the phenomenon of the stall flutter quite satisfactory (fig.8,9).

The second complex phenomenon of an aeroelastic instability which limits the maximum helicopter speed and the rotors speed is generally called a flutter. It is important to know the correspondence of the flutter boundaries in ground tests and in forward flight. The models developed ("ULYSS-6","FLAT", "ULMFE") satisfactory describe two types of instability: torsional flexure flutter at ground testing and transonic flutter in forward flight.

The results of the analysis (fig.10) show that the possible forms of flutter at ground testing correspond to the lower tone of the control linkage natural mode which is determined by the eigenvectors of the elasticity matrix (fig.3).

The study of flutter nature in forward flight showed that the determining factor is the static instability of NACA 23012 airfoil in respect to the angle of attack in the transonic range of Mach numbers 0.84-0.92. The most important practical conclusion was made that it is worthwhile to use TSAGI P5-5-11X airfoil in the aeroelastic blade layout.

On fig.11 it is shown that a substitution of NACA 23012 airfoil for TSAGI P5-5-11X airfoil in numerical xperiment brings about an elimination of flutter in a forward flight.

The main results of studying the coaxial-rotor system flutter are shown on fig.12 and permit to make the following conclusions:

- the use of TSAGI P5-5-11X airfoil increases the critical flutter speed not less than by 50 km/h according to the results of the numerical experiment and the flight tests confirm this estimation;

- lifting systems showing near flutter boundaries at ground testing may demonstrate essentially different flutter boundaries in a forward flight;

- the flutter boundary calculations satisfactory correspond to the results of ground as well as flight testing.

In numerical experiments on the basis of "ULYSS-6" model the problems of coaxial-rotor blades approach were examined. On fig.13 the results of the "ULYSS-6" calculations and their comparison with the flight experiment are shown: the influence of the structure design parameter, i.e. value of the flap regulator angle, on the approach of the coaxial-rotor blades. It is seen how important are the aeroelastic torsion deformations of the blade and the linkage, if this factor isn't taken into account the calculations shall not yield the current result.

In the numeric... experiments the depende... of the approach on the roll and pitch rates is clarified and confirmed. From the vector diagrams on fig.13 it may be seen that under the effect of the Coriolis forces twisting the blade there appear elastic deformations of the linkage and the blade which determine the flap motion and the approach. The calculated approach values quite satisfactorily correspond to the test results and are by several times in excess of the calculated approach of rigid blades.

To make a summary the following should be noted. The general mathematic model adequatly describing the variety of the aeroelastic phenomena on the stationary, unstationary and limiting flight modes was created. The correspondence of the calculations results to the results of the flight tests is determined by the set of the modeled factors.

On the basis of a generalized model the main problems of the coaxial-rotor lifting system aeroelasticity were examined and some principally new scientific results were obtained:

- the stall boundary of an elastic blade and of a coaxial-rotor lifting system was calculated;
- the nature of the transonic flutter was understood;
- the boundaries and the correspondence of the boundaries, the flutter forms in a forward flight and at ground testing were determined;
- the decisive influence of the aeroelastic torsion deformations on the flap motion and the blades approach was discovered.

4. THE FLIGHT SUPPORT AND ANALYSIS RESULTS

The questions concerning flight testing monitoring and the analysis of the results on the basis of the mathematical model are touched upon.

The use of the mathematic model on the design stage permits to properly choose the parameters of the blade aeroelastic layout. Development of the coaxial-rotor lifting system, planning and the analysis of the flight experiment are based on the general mathematic model.

In the process of the blade development an aeroelastic deformation of a airfoil trailing section was discovered. The numerical experiment using "ULYSS-1" model permited to evaluate the decrease of the alternating pitch link loads amplitude by increasing the rigidity of the trailing section by 2...3 times. The flight testing confirmed the value of the loads decrease after the modification of the trailing section (fig.14).

As the numerical experiment showed, the decrease of the torsional rigidity of the blade leads the flight experiment to the decrease of the alternating pitch link loads amplitude (fig.14) confirmed the prediction.

The flight testing fully confirmed the correctness of the decisions taken at the designing of a principally new lifting system. At flight experiments the influence of the aeroelastic layout parameters on the loads and vibration levels was examined and the aeroelastic layout of the blade was considerably improved (fig.15).

5. CONCLUSIONS

The fundamentals of the coaxial-rotor lifting systems aeroelasticity were worked out.

The general mathematical model was created which serves as a scientific base for numeric and flight studies and designing.

The principle new results on transonic flutter, stall flutter, blades approach of the coaxial helicopters were obtained.

The results of the studies permit to design the helicopter rotors with the desired parameters and to reduce the time periods of design and flight development.

COAXIAL ROTORS LIFTING SYSTEM AEROELASTICITY PROBLEMS

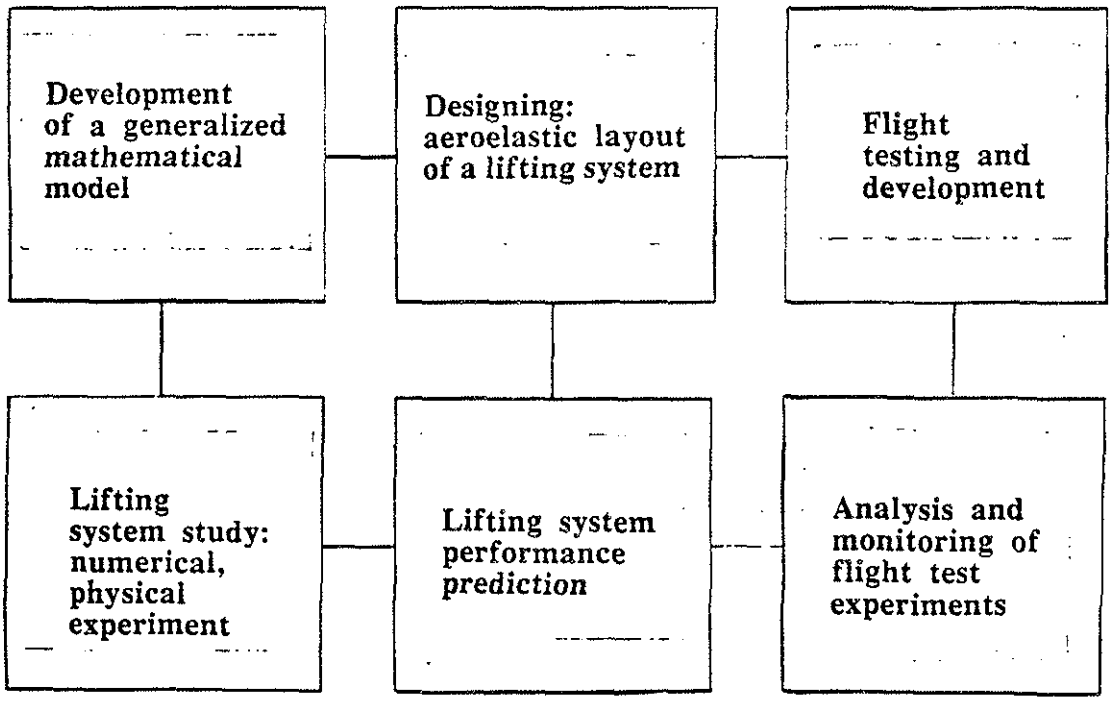

Fig. 1

MOTION EQUATIONS AND BOUNDARY CONDITIONS

$$m\left(\frac{\partial^2 y}{\partial t^2}+\sigma_T\frac{\partial^2\varphi}{\partial t^2}\right)=\frac{\partial}{\partial S}\left(N\frac{\partial}{\partial S}(y+\sigma_p\varphi)\right)-\frac{\partial}{\partial S}\left[(\sigma_T-\sigma_p)\varphi\frac{\partial N}{\partial S}\right]-$$

$$-\frac{\partial^2}{\partial S^2}\left\{\left[EJ_{y1}\cos^2\varphi+EJ_{x1}\sin^2\varphi\right]\frac{\partial^2\bar y}{\partial S^2}-\frac{1}{2}(EJ_{x1}-EJ_{y1})\frac{\partial^2\bar x}{\partial S^2}\sin 2\varphi\right\}+\frac{\partial y_A}{\partial S}\ ;$$

$$m\frac{\partial^2 x}{\partial t^2}=\frac{\partial}{\partial S}\left(N\frac{\partial}{\partial S}(x-\sigma_p)\right)+m\omega^2(x-\sigma_T)+\frac{\partial}{\partial S}\left[(\sigma_T-\sigma_p)\frac{\partial N}{\partial S}\right]+m\omega^2(\sigma_T-\sigma_p)+2m\omega\frac{\partial z_p}{\partial t}-\frac{\omega^2 m\ell}{S}(x-\sigma_T)$$

$$-\frac{\partial^2}{\partial S^2}\left\{\left[EJ_{x1}\cos^2\varphi+EJ_{y1}\sin^2\varphi\right]\frac{\partial^2\bar x}{\partial S^2}-\frac{1}{2}\left[EJ_{x1}-EJ_{y1}\right]\frac{\partial^2\bar y}{\partial S^2}\sin 2\varphi\right\}+\frac{\partial X_A}{\partial S}\ ;$$

$$(J_T+m\sigma_T^2)\frac{\partial^2\varphi}{\partial t^2}+m\sigma_T\frac{\partial^2 y}{\partial t^2}=\sigma_p\frac{\partial}{\partial S}\left[N\frac{\partial}{\partial S}(y+\sigma_p\varphi)\right]+(\sigma_T-\sigma_p)\frac{\partial(y+\sigma_p\varphi)}{\partial S}\frac{\partial N}{\partial S}-\omega^2(J_{y2}+m\sigma_T^2)\varphi$$

$$+\frac{\partial}{\partial S}\left(GJ\frac{\partial\bar\varphi}{\partial S}\right)+\frac{\partial^2\bar x}{\partial S^2}\frac{\partial^2\bar y}{\partial S^2}(EJ_{x1}-EJ_{y1})(1-2\sin^2\varphi)+\left[\left(\frac{\partial^2\bar x}{\partial S^2}\right)^2-\left(\frac{\partial^2\bar y}{\partial S^2}\right)^2\right]\left[EJ_{x1}-EJ_{y1}\right]\frac{1}{2}\sin 2\varphi+\frac{\partial M_A}{\partial S};$$

$$\varphi(0,t)=\varphi_0+B_1\cos\Psi+B_2\sin\Psi-\bar K\frac{\partial y}{\partial S}(0,t)+\vartheta_{\Psi 1}\left[GJ_0\frac{\partial\bar\varphi}{\partial S}(0,t)-M_{TP}^{\omega_1}(t)\right];\quad \frac{\partial^2\bar x}{\partial S^2}(R,t)=\frac{\partial^2\bar y}{\partial S^2}(R,t)=0;$$

$$y(0,t)=0\ ;$$

$$\left[EJ_{y1}\cos^2\varphi+EJ_{x1}\sin^2\varphi\right]\frac{\partial^2\bar y}{\partial S^2}-\frac{1}{2}\sin 2\varphi\left[EJ_{x1}-EJ_{y1}\right]\frac{\partial^2\bar x}{\partial S^2}=M_{TP}^{\omega_1}-\bar K\left[GJ_0\frac{\partial\bar\varphi}{\partial S}(0,t)-M_{TP}^{\omega_1}\right];\ \frac{\partial^3\bar x}{\partial S^3}(R,t)=\frac{\partial^3\bar y}{\partial S^3}(R,t)=0;$$

$$x(0,t)=0\ ;$$

$$\left[EJ_{x1}\cos^2\varphi+EJ_{y1}\sin^2\varphi\right]\frac{\partial^2\bar x}{\partial S^2}-\frac{1}{2}\sin 2\varphi\left[EJ_{x1}-EJ_{y1}\right]\frac{\partial^2\bar y}{\partial S^2}=M_{TP}^{\omega_1}(t)\ ;\qquad \frac{\partial\bar\varphi}{\partial S}(R,t)=0;$$

EXPERIMENT — ROTORS CONTROL LINKAGE MODEL

the scheme of experiment on determination of the control linkage elasticity matrix

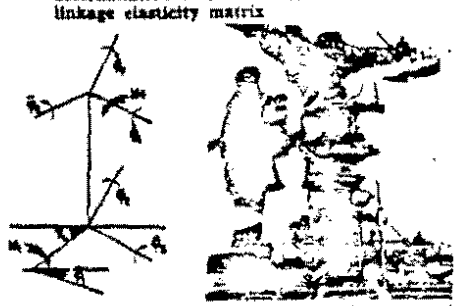

rotors control linkage models

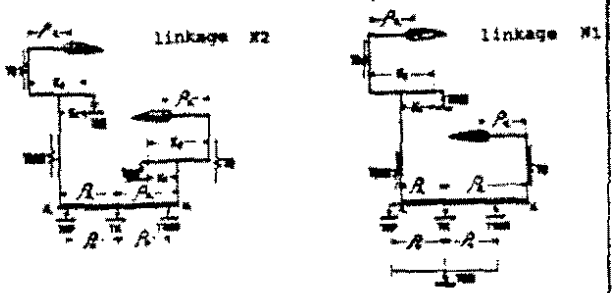

$$\begin{Vmatrix}\varphi_1\\ \varphi_2\\ \varphi_3\\ \varphi_4\\ \varphi_5\\ \varphi_6\end{Vmatrix} = \left\|\begin{array}{ccc|ccc} \sigma_{11} & \sigma_{12} & \sigma_{13} & \sigma_{14} & \sigma_{15} & \sigma_{16}\\ \sigma_{21} & \sigma_{22} & \sigma_{23} & \sigma_{24} & \sigma_{25} & \sigma_{26}\\ \sigma_{31} & \sigma_{32} & \sigma_{33} & \sigma_{34} & \sigma_{35} & \sigma_{36}\\ \hline \sigma_{41} & \sigma_{42} & \sigma_{43} & \sigma_{44} & \sigma_{45} & \sigma_{46}\\ \sigma_{51} & \sigma_{52} & \sigma_{53} & \sigma_{54} & \sigma_{55} & \sigma_{56}\\ \sigma_{61} & \sigma_{62} & \sigma_{63} & \sigma_{64} & \sigma_{65} & \sigma_{66} \end{array}\right\| \times \begin{Vmatrix} M_1\\ M_2\\ M_3\\ M_4\\ M_5\\ M_6 \end{Vmatrix}$$

ELASTICITY MATRIX

APPROXIMATION:

$$\sigma_{ij}(\psi_{1L}) = f(T_0, T_{1K}, T_{1KK}, T_{0K}, T_{1KK}, T_{1KK}, T_{1KK}, \psi_{1L});$$

CALCULATION:

$$\sigma_{ij}(\psi_{1L}) = \frac{KA_i}{\rho_{ij}}\cdot\frac{KA_{ij}}{\rho_{ij}}\left\{T_0\left[KA_i(\sin\varphi_i+\cos\varphi_i)-1\right]\left[KA_j(\sin\varphi_j+\cos\varphi_j)-1\right]\right.$$
$$\left.+KA_i\cdot KA_j\left(T_{1KK}\cos\varphi_i\cos\varphi_j+T_{0K}\sin\varphi_i\sin\varphi_j\right)\right\}+T_0+T_{1KK}+\sigma_{ij_0};$$

$$\sigma_0 = \left\|\begin{array}{cc} T_{0K} & 2T_{0K}\\ 2T_{0K} & 4T_{0K}+T_{1KK}\end{array}\right\|;$$

$$\varphi_l = \begin{cases} \psi_{1L}+\Omega\Pi-\dfrac{\pi}{2}-\dfrac{2\pi}{K}(l-1); & l=1,2,\ldots,K\\ 2\pi-(\psi_{1L}+\Omega\Pi+\Delta F)\dfrac{\pi}{2}-\dfrac{2\pi}{K}(l-K-1); & l=K+1,\ldots,2K\end{cases}$$

main rigidities of the elasticity matrix and dynamic rigidities obtained at frequency testing

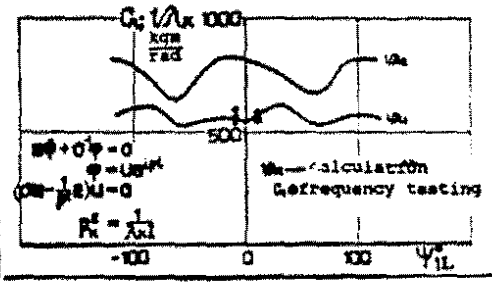

Fig. 3

NONSTATIONARY BLADE AERODYNAMICS

3-D "STRAP THEORY", THE STREAM IS NORMAL TO THE 1/4 CHORDS LINE

airfoil characteristics in stationary stream (α^*, M^*)

$C_y, C_{xp}, C_m(\alpha_\infty, M) = C_y, C_{xp}, C_m(\alpha^*, M^*)$

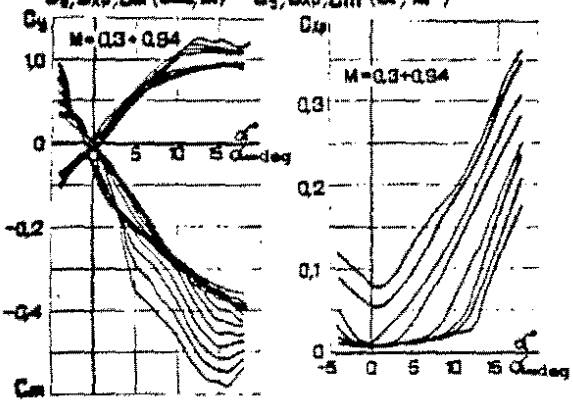

$C_m(C_y, M)$ for aeroelastic and rigid airfoil

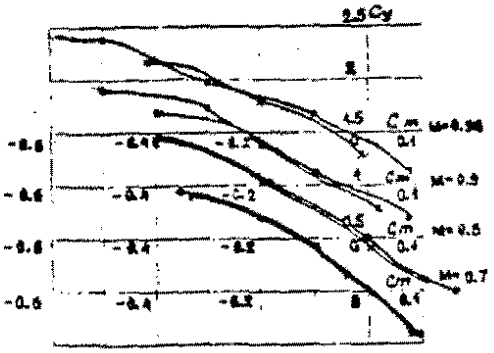

dynamic stall $\alpha^* = f(\alpha_\infty, \dot{\alpha}, M_N)$

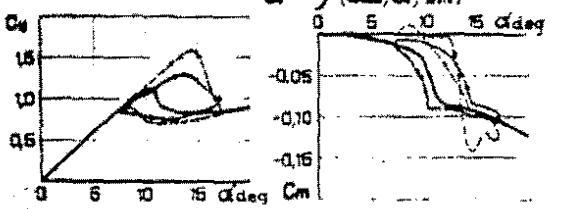

aeroelastic deformations of the trailing section

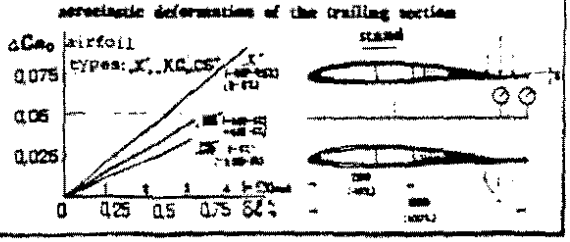

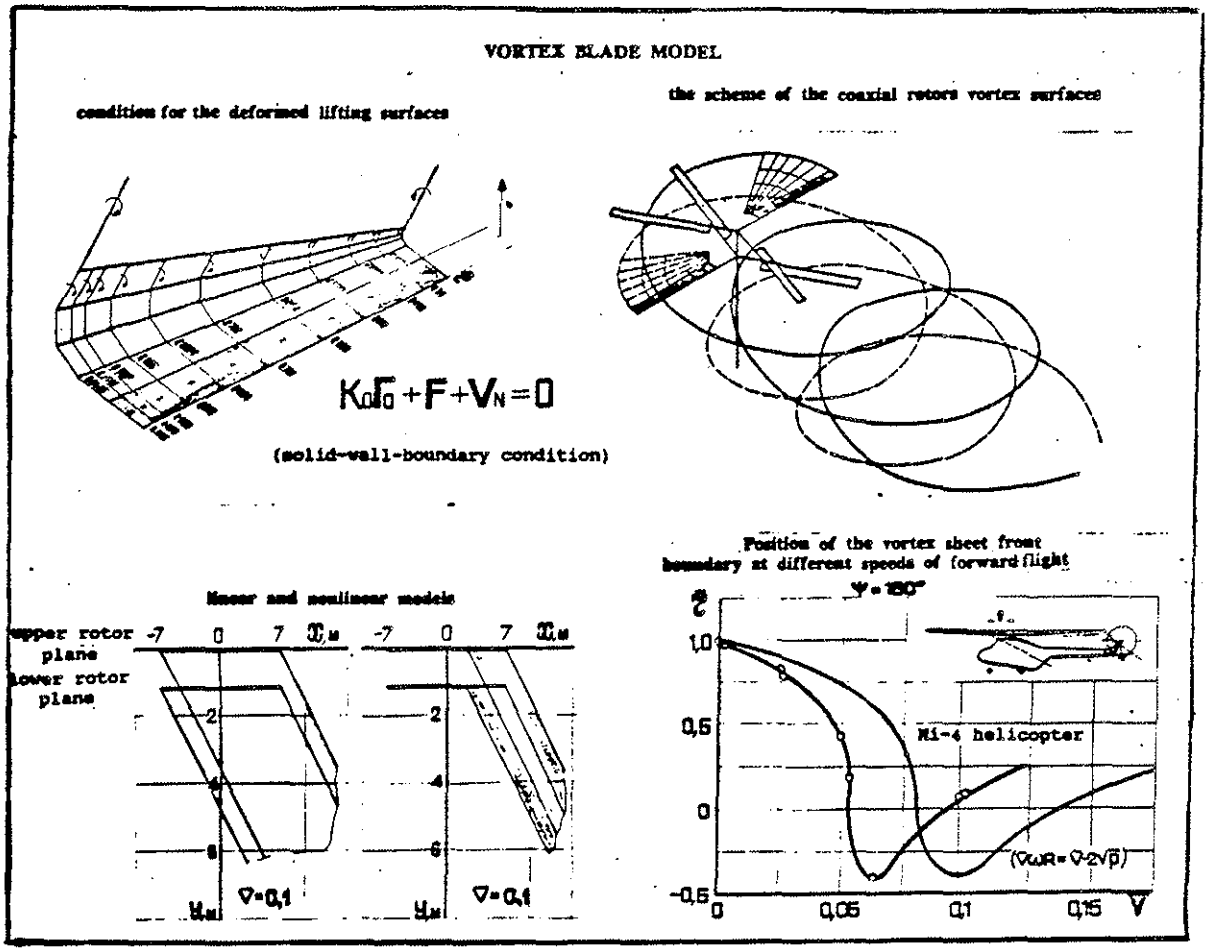
VORTEX BLADE MODEL
condition for the deformed lifting surfaces
$K_0\Gamma_0 + F + V_N = 0$
(solid-wall-boundary condition)
the scheme of the coaxial rotors vortex surfaces
Linear and nonlinear models
upper rotor plane
lower rotor plane
$\bar{y}_M$
$\nabla = 0,1$
Position of the vortex sheet front boundary at different speeds of forward flight
$\Psi = 180°$
Mi-4 helicopter
$(\nabla_\omega R = \nabla + 2\sqrt{\mu})$
$\bar{z}$
$\bar{x}$

Fig. 5

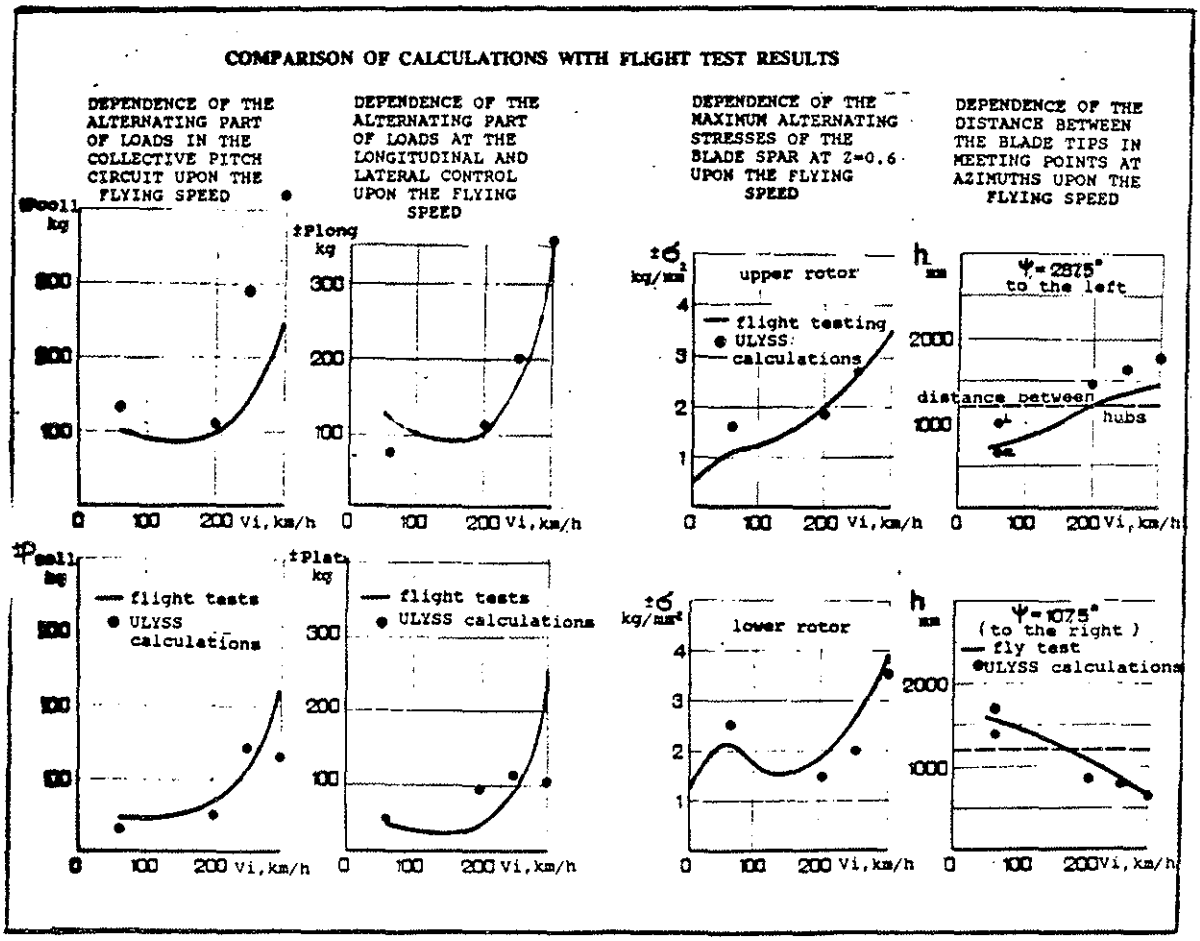
COMPARISON OF CALCULATIONS WITH FLIGHT TEST RESULTS
DEPENDENCE OF THE ALTERNATING PART OF LOADS IN THE COLLECTIVE PITCH CIRCUIT UPON THE FLYING SPEED
DEPENDENCE OF THE ALTERNATING PART OF LOADS AT THE LONGITUDINAL AND LATERAL CONTROL UPON THE FLYING SPEED
DEPENDENCE OF THE MAXIMUM ALTERNATING STRESSES OF THE BLADE SPAR AT Z=0.6 UPON THE FLYING SPEED
DEPENDENCE OF THE DISTANCE BETWEEN THE BLADE TIPS IN MEETING POINTS AT AZIMUTHS UPON THE FLYING SPEED
upper rotor
lower rotor
flight testing
ULYSS calculations
flight tests
$\Psi = 287.5°$ to the left
$\Psi = 107.5°$ (to the right)
distance between hubs
fly test
Vi, km/h

FUNCTIONAL CAPABLITIES AND MODELED FACTORS

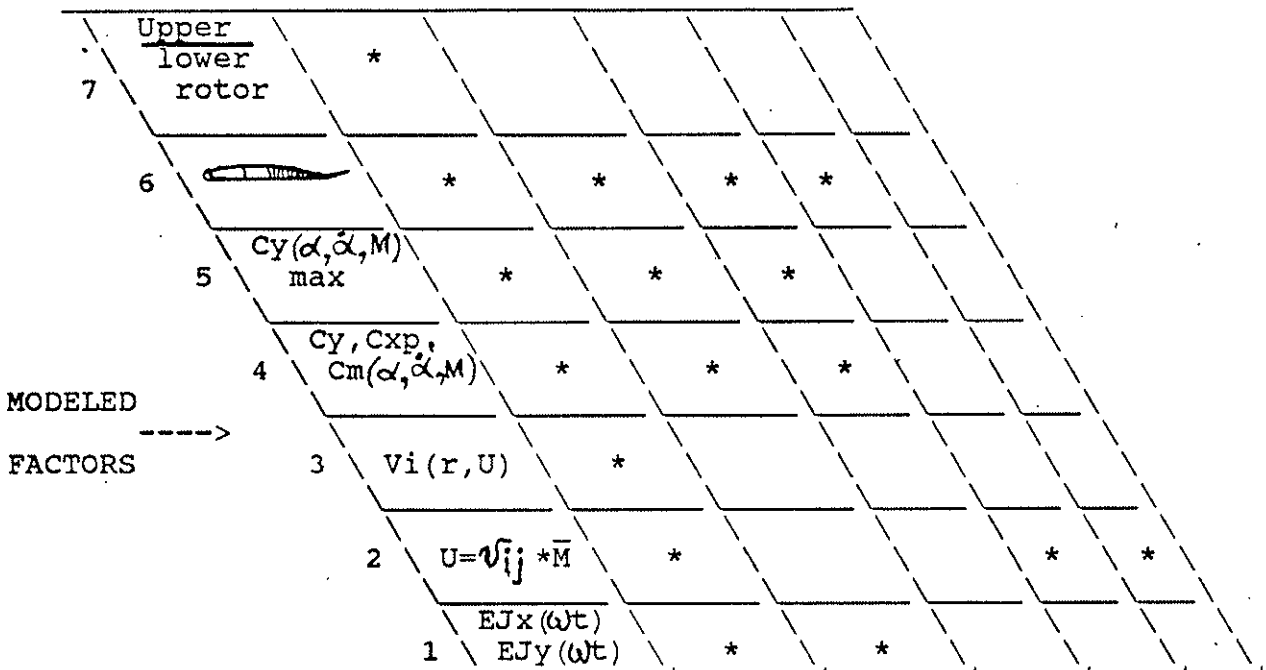

ANALYSIS RESULT	MODEL VERSION	ULYSS-6	ULYSS-1	ULMFE	FLAT	MFE
1	Stall flutter boundary	CRLS	B	B		
2	Bending and pitch link loads	CRLS	B	B		
3	Buster loads, blade elastic deformations	CRLS	B	B		
4	Hub alternating forces and moments	CRLS	B	B		
5	Blade tips approach	CRLS				
6	Flutter in forward flight	CRLS	B	B		
7	Flutter in ground tests	CRLS			B	
8	Natural frequences			B	B	B

Notes: CRLS - Coaxial-Rotor Lifting System, B - Blade.

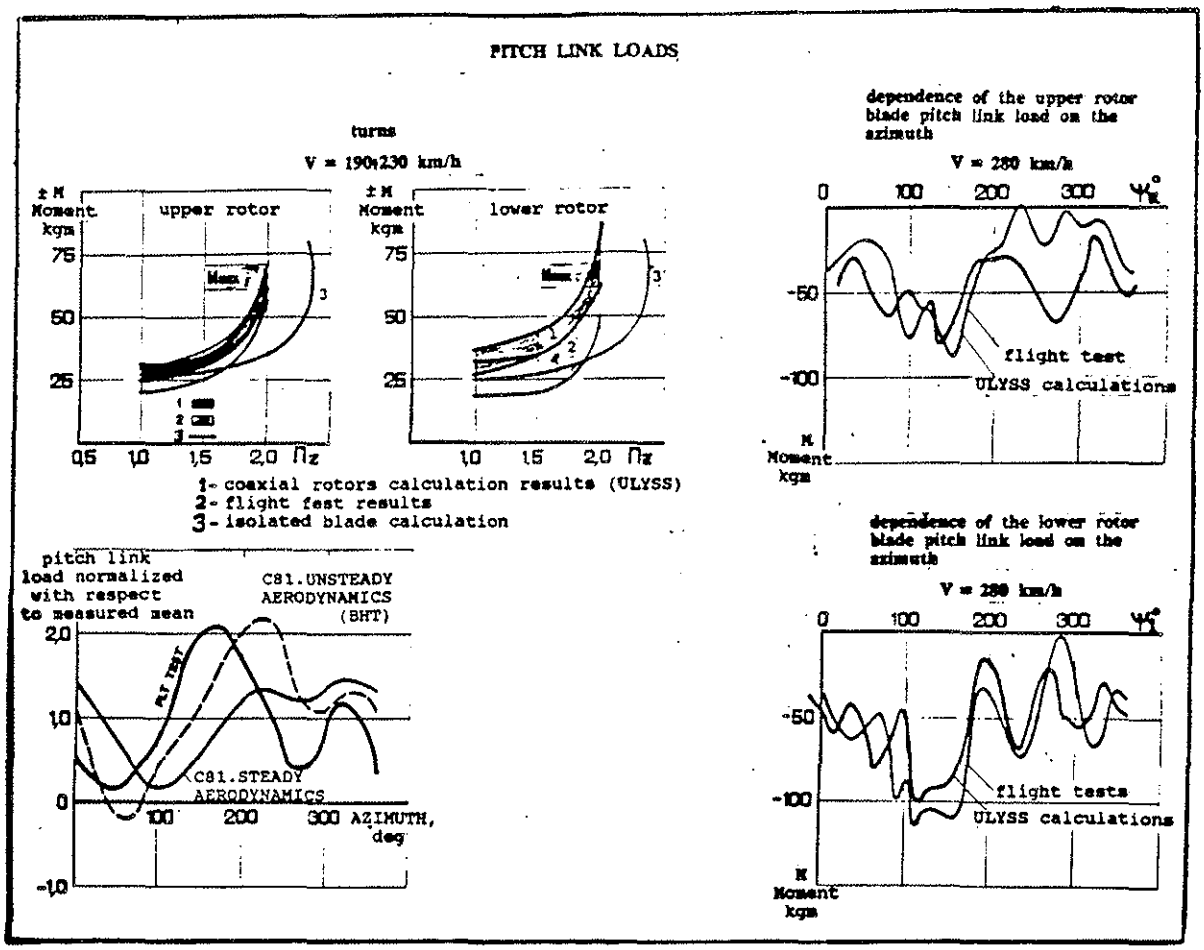
PITCH LINK LOADS
turns
V = 190÷230 km/h
± M Moment kgm
upper rotor
lower rotor
75
50
25
0,5 1,0 1,5 2,0 nz
1- coaxial rotors calculation results (ULYSS)
2- flight fest results
3- isolated blade calculation
dependence of the upper rotor blade pitch link load on the azimuth
V = 280 km/h
0 100 200 300 ψ°
-50
-100
flight test
ULYSS calculations
M Moment kgm
dependence of the lower rotor blade pitch link load on the azimuth
V = 280 km/h
flight tests
ULYSS calculations
pitch link load normalized with respect to measured mean
CS1.UNSTEADY AERODYNAMICS (BHT)
FLT TEST
CS1.STEADY AERODYNAMICS
2,0
1,0
0
-1,0
100 200 300 AZIMUTH, deg

Fig. 8

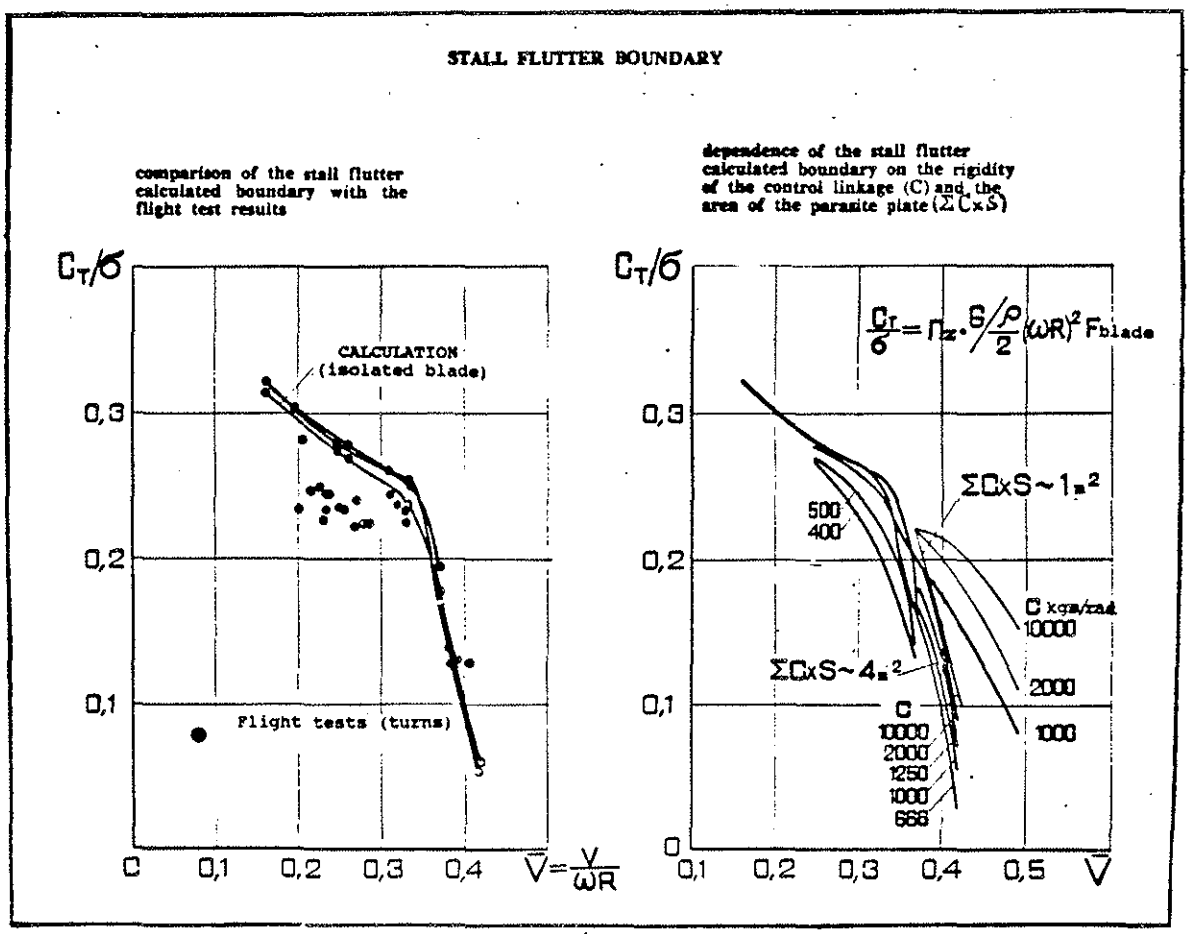
STALL FLUTTER BOUNDARY
comparison of the stall flutter calculated boundary with the flight test results
dependence of the stall flutter calculated boundary on the rigidity of the control linkage (C) and the area of the parasite plate (ΣCxS)
CT/σ
CALCULATION (isolated blade)
Flight tests (turns)
0,3
0,2
0,1
0
0,1 0,2 0,3 0,4
V̄ = V/ωR
CT/σ = nz · S/ρ/2 (ωR)² Fblade
ΣCxS ~ 1 m²
ΣCxS ~ 4 m²
500
400
C kgm/rad
10000
2000
1000
C
10000
2000
1250
1000
666
0,1 0,2 0,3 0,4 0,5 V̄

Fig. 9

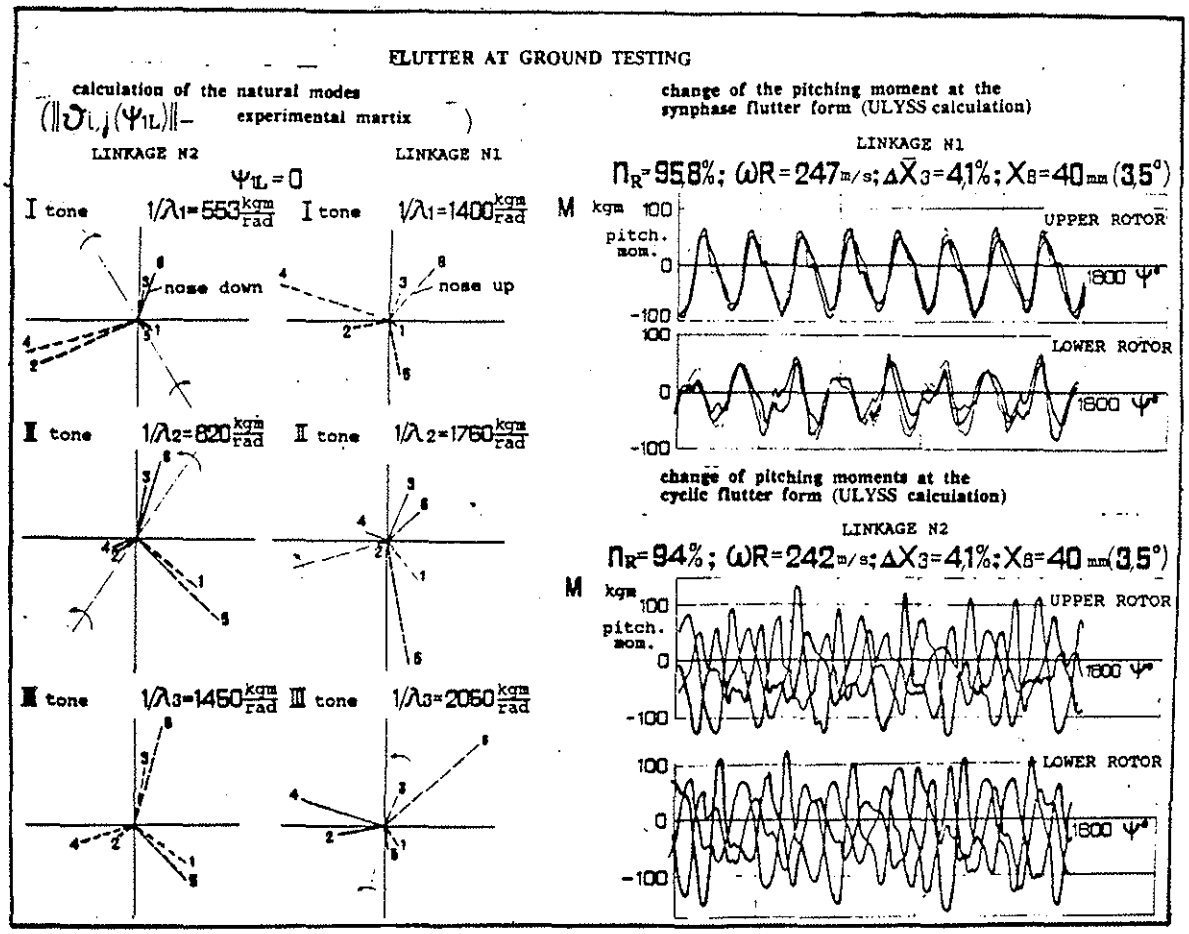
FLUTTER AT GROUND TESTING
calculation of the natural modes
experimental martix
LINKAGE N2
LINKAGE N1
$\Psi_{1L}=0$
I tone $1/\lambda_1=553\frac{kgm}{rad}$
I tone $1/\lambda_1=1400\frac{kgm}{rad}$
nose down
nose up
I tone $1/\lambda_2=820\frac{kgm}{rad}$
II tone $1/\lambda_2=1760\frac{kgm}{rad}$
III tone $1/\lambda_3=1450\frac{kgm}{rad}$
III tone $1/\lambda_3=2050\frac{kgm}{rad}$
change of the pitching moment at the synphase flutter form (ULYSS calculation)
LINKAGE N1
$\Pi_R=95.8\%$; $\omega R=247$ m/s; $\Delta\bar{X}_3=4.1\%$; $X_B=40$ mm (3.5°)
M kgm
pitch. mom.
UPPER ROTOR
LOWER ROTOR
1800 Ψ°
change of pitching moments at the cyclic flutter form (ULYSS calculation)
LINKAGE N2
$\Pi_R=94\%$; $\omega R=242$ m/s; $\Delta X_3=4.1\%$; $X_B=40$ mm (3.5°)

Fig. 10

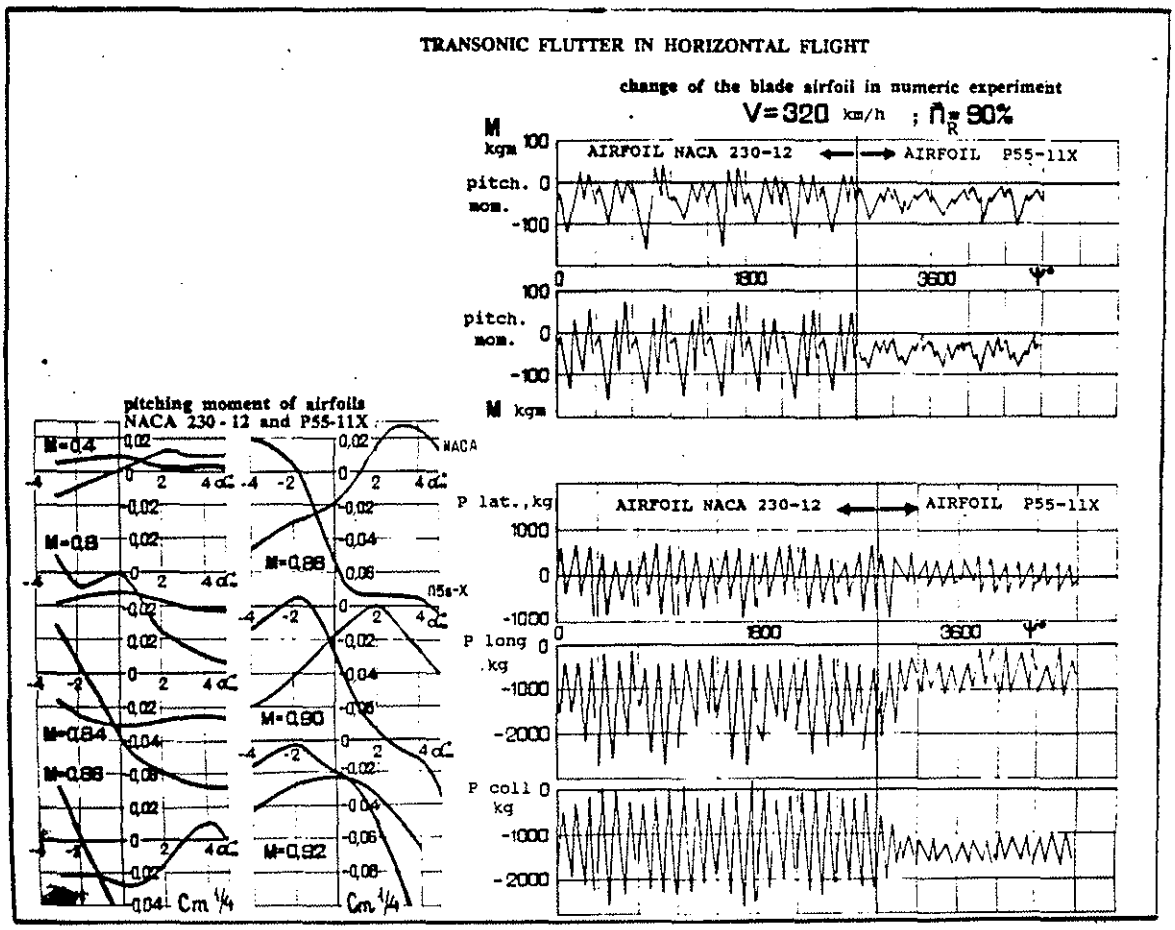
TRANSONIC FLUTTER IN HORIZONTAL FLIGHT
change of the blade airfoil in numeric experiment
V=320 km/h ; Π_R=90%
M kgm
pitch. mom.
AIRFOIL NACA 230-12
AIRFOIL P55-11X
1800
3600
Ψ°
P lat., kg
P long kg
P coll kg
pitching moment of airfoils NACA 230-12 and P55-11X
M=0.4
M=0.8
M=0.84
M=0.88
M=0.86
M=0.90
M=0.92
NACA
05s-X
Cm ¼

Fig. 11

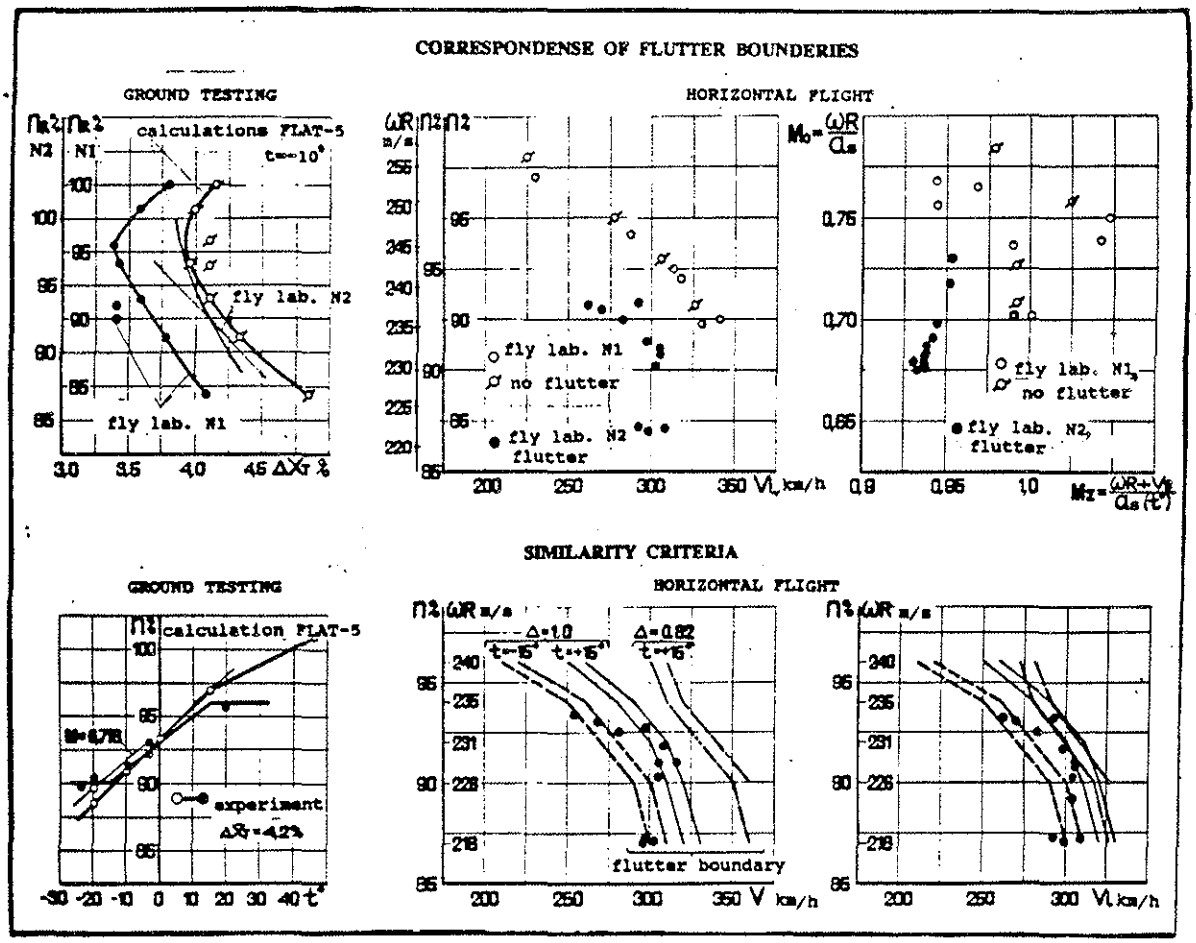
CORRESPONDENSE OF FLUTTER BOUNDERIES
GROUND TESTING
HORIZONTAL FLIGHT
calculations FLAT-5
fly lab. N2
fly lab. N1
no flutter
flutter
SIMILARITY CRITERIA
calculation FLAT-5
experiment
flutter boundary

Fig. 12

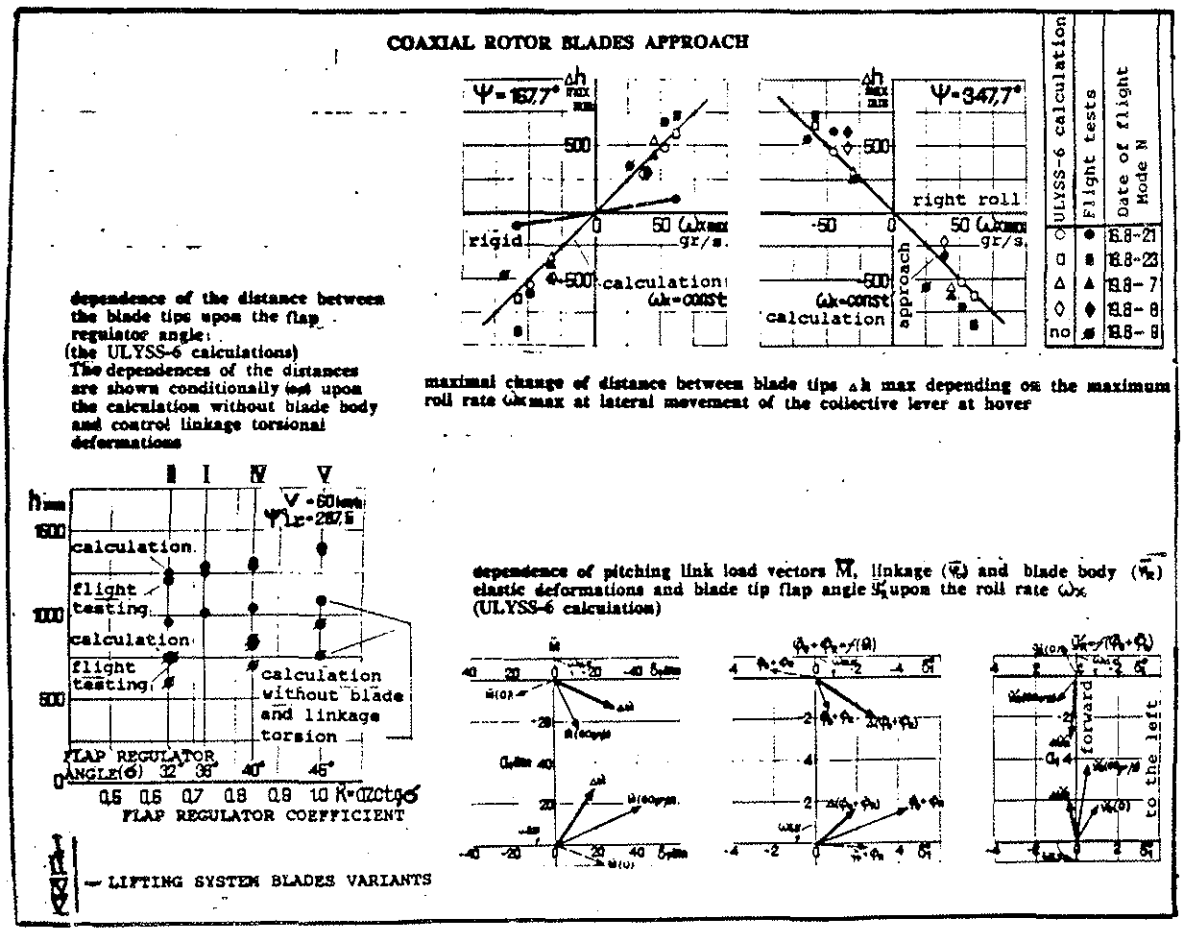
COAXIAL ROTOR BLADES APPROACH
rigid
calculation
right roll
approach
ULYSS-6 calculation
Flight tests
Date of flight
Mode N
dependence of the distance between the blade tips upon the flap regulator angle:
(the ULYSS-6 calculations)
The dependences of the distances are shown conditionally (not) upon the calculation without blade body and control linkage torsional deformations
maximal change of distance between blade tips Δh max depending on the maximum roll rate ωx max at lateral movement of the collective lever at hover
calculation
flight testing
calculation without blade and linkage torsion
FLAP REGULATOR ANGLE(δ)
FLAP REGULATOR COEFFICIENT
dependence of pitching link load vectors, linkage and blade body elastic deformations and blade tip flap angle upon the roll rate ωx (ULYSS-6 calculation)
forward
to the left
— LIFTING SYSTEM BLADES VARIANTS

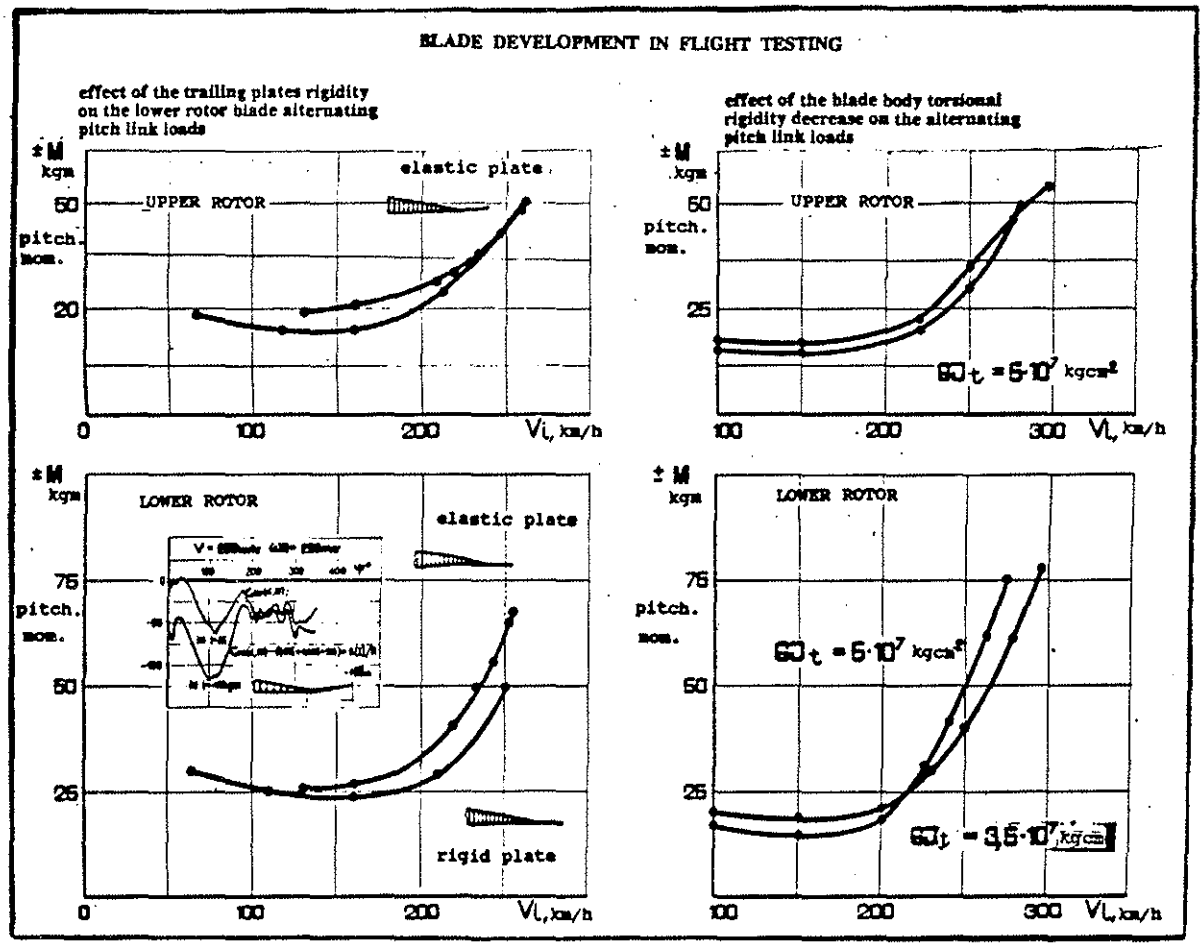
BLADE DEVELOPMENT IN FLIGHT TESTING
effect of the trailing plates rigidity on the lower rotor blade alternating pitch link loads
±M kgm
pitch. mom.
UPPER ROTOR
elastic plate
50
20
0
100
200
Vi, km/h
effect of the blade body torsional rigidity decrease on the alternating pitch link loads
UPPER ROTOR
25
GJt = 5·10⁷ kgcm²
300
LOWER ROTOR
elastic plate
rigid plate
75
GJt = 3,5·10⁷ kgcm²

Fig. 14

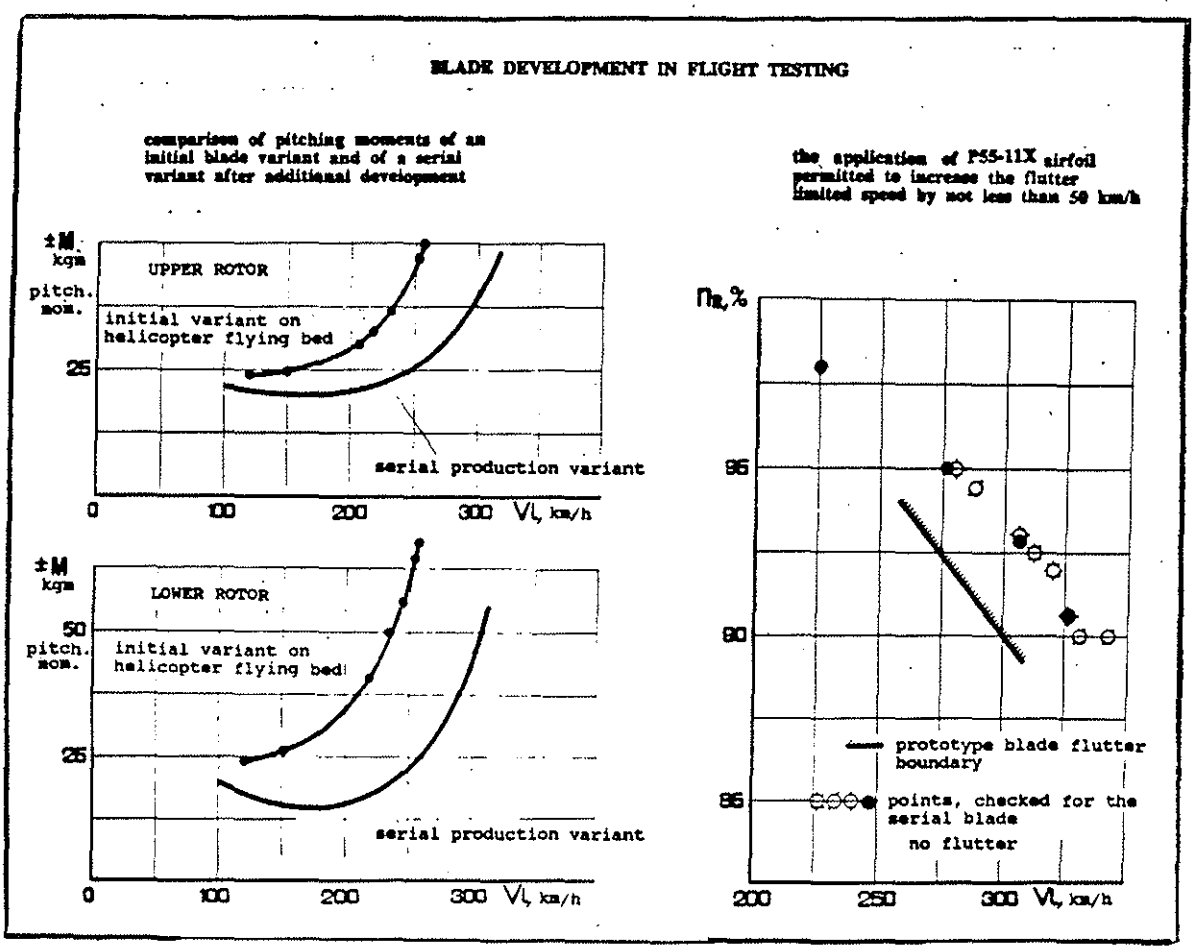
BLADE DEVELOPMENT IN FLIGHT TESTING
comparison of pitching moments of an initial blade variant and of a serial variant after additional development
±M kgm
pitch. mom.
UPPER ROTOR
initial variant on helicopter flying bed
serial production variant
25
0
100
200
300
Vi, km/h
LOWER ROTOR
50
the application of P55-11X airfoil permitted to increase the flutter limited speed by not less than 50 km/h
Mm,%
95
90
85
prototype blade flutter boundary
points, checked for the serial blade
no flutter
250